

Cite this: *Green Chem.*, 2011, **13**, 1819

www.rsc.org/greenchem

PAPER

A catalytic route to lower alcohols from glycerol using Ni-supported catalysts

Esti van Ryneveld,^a Abdul S. Mahomed,^b Pieter S. van Heerden,^b Mike J. Green^c and Holger B. Friedrich^{*a}

Received 22nd November 2010, Accepted 28th March 2011

DOI: 10.1039/c0gc00839g

The activity of Ni-supported catalysts on silica and alumina was studied for the transformation of glycerol to lower alcohols, primarily 1-propanol and ethanol. Pressure had a small effect on glycerol conversion whereas temperature had a significant effect on conversion and selectivity. Ni/SiO₂ gave quantitative conversion of glycerol at a lower temperature compared to Ni/Al₂O₃. Ni/SiO₂ also gave a higher selectivity to ethanol and propanol (63%) compared to Ni/Al₂O₃ (52%) at a similar conversion. The higher activity of Ni/SiO₂ can be ascribed to its smaller crystallite size ascertained from XRD analysis. The Ni/SiO₂ catalyst also showed improved reducibility compared to Ni/Al₂O₃. The used catalyst showed sintering of the Ni, which was confirmed by a loss of surface area and average crystallite size. The route to lower alcohols from glycerol is proposed to occur *via* 1,2-propanediol. Biomass is readily converted into biodiesel and glycerol and we have developed a route to convert glycerol into lower alcohols. We have therefore demonstrated that it is possible to convert biomass into biodiesel and lower alcohols (*via* glycerol) from the same crop, thus reducing the need to produce ethanol from a separate government-subsidised crop.

1. Introduction

The interest in the catalytic conversion of renewable feedstocks to a range of value-added chemical commodities has been increasing. Studies on the hydrogenolysis of polyhydric alcohols have been pursued since 1930. Glycerol is an important building block in natural fats and oils,¹ and recently the need has arisen to find new applications for this by-product obtained from the production of biodiesel. Glycerol can be converted to hydrogen and synthesis gas by reforming,² to 1,2-propanediol (1,2-PDO), 1,3-propanediol (1,3-PDO) and ethylene glycol (EG) *via* hydrogenolysis,³ and also to lower alcohols such as methanol, ethanol, 1-propanol and 2-propanol.⁴

Much work has been done towards the hydrogenolysis of glycerol to 1,3- and 1,2-PDO, as well as oxidation of glycerol to glyceric acid or dihydroxyacetone.⁵ However, routes to lower alcohols, such as 1-propanol and ethanol, have been less discussed. It is known that glycerol can be hydrogenolysed using various heterogeneous systems including Rh, Ru, Pt,

PtRu, copper systems and Raney[®] Ni.⁶ Surprisingly, the use of supported Ni systems as catalysts towards the chemical transformation of glycerol, especially towards the formation of lower alcohols, has appeared less frequently in the literature.^{7–11}

Bloom⁷ described a process for the hydrogenolysis of a 40 wt% glycerol feedstock. Several Ni-supported catalysts were used, and the major product was 1,2-PDO with a selectivity of up to 72%. The supports that were used include carbon, silica and alumina.

The hydrogenolysis of polyols (*e.g.* xylitol, sorbitol or glycerol) to ethylene glycol in the presence of nickel on silica (or nickel on alumina) and hydrogen was described by Bullock *et al.*⁸ High conversions were observed, with 70% selectivity to 1,2-PDO, 15% to ethylene glycol (EG), and 11% of degradation products.

Huang *et al.*⁹ reported on the hydrogenolysis of solvent-free glycerol to 1,2-PDO. Several catalysts were screened and the most effective catalysts (41 wt% Ni/Al₂O₃ and 32 wt% Cu/ZnO/Al₂O₃) were further tested for vapour-phase hydrogenolysis in a fixed bed. They found that Ni/Al₂O₃ is not an effective catalyst for the production of 1,2-PDO because of the high selectivity to CH₄ and CO.

The catalytic hydrogenolysis of glycerol to propanediols using homogeneous Pd and Pt systems was also described by Drent and Jager.¹⁰ Typical selectivities obtained were 47% to 1-propanol, 31% to 1,3-PDO and 22% to 1,2-PDO. The hydrogenolysis was carried out under moderate reaction

^aSchool of Chemistry, University of KwaZulu-Natal, Westville Campus, Private Bag X54001, Durban, 4000, South Africa.
E-mail: friedric@ukzn.ac.za; Fax: +27 31-2603109; Tel: +27 31-2603107

^bSasol Technology, R&D, 1 Klasie Havenga Street, Sasolburg, 1948, South Africa

^cSchool of Chemistry, Newcastle University, Bedson Building, Newcastle upon Tyne, NE1 7RU, UK

conditions with temperatures in the range of 140 °C and pressures around 40 bar H₂.

Tomishige and co-workers¹¹ reported a high selectivity of 42% to 1-propanol and 13% to 2-propanol using supported metal catalysts (Rh, Ru, Pt, Pd on active carbon, SiO₂, Al₂O₃) during the hydrogenolysis of aqueous glycerol solutions under H₂ in a batch reactor.

Thus, much of the work that has been reported focused on the production of 1,2-propanediol from glycerol using Cu supported systems, and at times, Ni catalysts. The focus of this work was the production of lower alcohols, primarily 1-propanol and ethanol, from glycerol using Ni-supported catalysts in a continuous flow fixed bed reactor.

The global capacity for 1-propanol is about 275 kt, and it is produced *via* the hydroformylation of ethylene to form propanal, which is then hydrogenated to 1-propanol.¹² Currently, 1-propanol is a fairly expensive commodity chemical and is mainly used as a solvent or in making *n*-propyl acetate.

The world production of ethanol in 2007 was about 52 Mt, and the average annual growth rate for ethanol for 2008–2013 is estimated at 9%.¹³ The primary source of ethanol is *via* the fermentation of sugar and grain crops (70% of global production), and the main market for ethanol is for fuel (80–90%).¹³

The price of refined glycerol has shown a significant decline over the last 5–7 years, and indeed a glycerol “lake” is being produced as a by-product of biodiesel (15 Mt p.a. in 2010, growing at around 10% p.a.; and 1 ton of glycerine is produced for every 10 tons of biodiesel). Between 2004 and 2007, the world capacity for refined glycerol grew at an average annual rate of 8.7%, faster than world consumption.¹⁴ Biomass is readily converted to biodiesel and glycerol, and we are therefore proposing a route to convert the low-value glycerol to high-value commodity alcohols, which also reduces the need to produce ethanol from a separate government-subsidised crop, thus freeing up land for food production.

2. Experimental

2.1 Reagents

The Ni/Al₂O₃ and Ni/SiO₂ catalyst systems were obtained as commercial samples in a partially reduced state. The average Ni content was between 45–55 wt% for Ni/Al₂O₃ and Ni/SiO₂ respectively. The glycerol was purchased from Sigma Aldrich and used without further purification. The glycerol feed was prepared as 60 wt% solution in water.

2.2 Catalyst characterisation

The BET surface areas were measured by nitrogen physisorption isotherms at 77 K using the standard multipoint method (eleven points) on a Micromeritics Gemini instrument. Prior to the analysis, samples were degassed in a stream of nitrogen at 473 K for 24 h.

Temperature-programmed reduction (TPR) and NH₃ temperature-programmed desorption (TPD) experiments were carried out in a Micromeritics 2900 AutoChem II Chemisorption Analyzer. Prior to the reduction in the TPR, the catalyst was pretreated by being heated under a stream of argon (30 ml min⁻¹)

at 350 °C for 30 min and then cooled down to 80 °C under the same stream of argon. In the reduction experiment, 5% H₂ in argon was used as a reducing agent at a flow rate of 50 ml min⁻¹. Under these reducing conditions, the temperature was ramped up to 950 °C at a rate of 10 °C min⁻¹.

In the TPD experiments, the catalysts (*ca.* 20 mg) were first reduced under 5% H₂ in argon and thereafter treated with helium for one hour to remove excess hydrogen. A 4% ammonia-in-helium gas mixture was then passed (20 ml min⁻¹) over the catalyst for 30 min. The excess ammonia was removed by flushing the system with helium (30 ml min⁻¹) for 30 min and then adsorbed ammonia was stripped off by the same stream of helium (30 ml min⁻¹) and a temperature ramp of up to 900 °C (at 10 °C min⁻¹). The desorption profiles were recorded using a TCD.

Powder X-ray diffraction patterns were recorded on a Bruker D8 Advance diffractometer equipped with a graphite monochromator and operated at 40 kV and 40 mA. The source of radiation was Co K α . 2θ covered the range between 10 and 90° at a speed of 1° min⁻¹ with a step size of 0.02°, and all data were evaluated with DIFFRACPLUS (EVA, SEARCH, TOPAS) software. Employing the peak at 50°, the average crystallite size was calculated using the Scherrer equation.

Scanning electron microscopy (SEM) images were obtained using a LEO 1450 Scanning Electron Microscope. Samples for SEM images were coated with gold using a Polaron SC Sputter Coater.

Transmission electron microscopy (TEM) images were taken on a Jeol JEM 1010 transmission electron microscope operated at a voltage of 100 kV. Samples were prepared by deposition of a small amount of the catalyst between two formvar-coated copper grids, and the images were captured with the MegaView III Soft Imaging System.

Thermogravimetric analysis–differential scanning calorimetry (TGA–DSC) was performed on the catalysts under a nitrogen atmosphere using a SDT Q 600 TGA–DSC instrument. The temperature was increased from room temperature to 1000 °C at a rate of 20 °C min⁻¹.

2.3 Catalytic testing

The catalytic reaction of glycerol was performed in a continuous flow fixed-bed reactor in down-flow mode. The reactor tube was stainless steel with an internal diameter of 20 mm and a length of 250 mm. The catalyst volume was 5 ml (*ca.* 8.5 g) and mixed with an equal amount of carborundum. The catalyst had a particle size distribution of 300–500 μ m. The molar ratio of hydrogen to glycerol solution was 2 : 1 with a GHSV of 1060 h⁻¹ and a LHSV of 3.0 h⁻¹. The catalytic reactions were carried out between 230–320 °C with pressures varying between 40–75 bar. Prior to the reaction, the catalyst was reduced at 180 °C after which the reactor was adjusted to operating conditions. The liquid products and the unreacted glycerol were collected in catchpots cooled to 3 °C and –20 °C respectively. The liquid products as well as the gas products were collected at regular intervals, and were analyzed on a GC (HP 6890) equipped with a FID using a DB-1701 column. Another gas sample was injected on a GC equipped with a TCD (Agilent 6850) using a Shincarbon-packed

Table 1 Textural properties of Ni-supported catalysts

Catalyst	BET surface area (m ² g ⁻¹)	Crystallite size from XRD (nm)	Degree of reducibility (%)
Fresh Ni/Al ₂ O ₃	150.5	17.7	51.4
Fresh Ni/SiO ₂	133.4	12.1	78.9
Used Ni/Al ₂ O ₃	21.5	31.5	—
Used Ni/SiO ₂	12.9	82.2	—

column for CH₄ and CO_x evaluation. Mass balances were 100 ± 5%.

3. Results and discussion

3.1 Catalyst characterisation

3.1.1 BET surface area. Table 1 compiles the BET specific surface area of the fresh and used Ni-supported catalysts. Results showed that the surface area for the Ni/Al₂O₃ was about 15% higher than Ni/SiO₂. As observed from the data, there is a significant decrease in surface area between the fresh and used catalysts. This decrease can probably be attributed to the sintering of the reduced Ni particles which is caused by high temperatures and the nature of the liquid phase of the reaction which can result in carbon deposits on the catalyst surface.¹⁵ This was also confirmed by XRD, for which Ni/SiO₂ showed crystallite size growth from 12 nm to 81 nm to form agglomerates. The sintering of the Ni particles on the support can contribute to the deactivation of the catalyst, due to the reduction of the accessible catalytic surface and the blocking of pores.¹⁶

3.1.2 Powder X-ray diffraction. Fig. 1 illustrates the diffractograms obtained for the fresh Ni/Al₂O₃ and the used Ni/Al₂O₃ catalysts. The XRD patterns for the fresh Ni/Al₂O₃ catalyst shows NiO lines at $2\theta = 37.3$ ($d = 2.35$), 44.3 ($d = 2.09$) and 62.9 ($d = 1.45$) confirming the presence of “free” nickel oxide.²⁰

The used Ni/Al₂O₃ catalyst showed peaks with $2\theta = 44.5$ ($d = 2.03$), 51.8 ($d = 1.76$), 76.3 ($d = 1.25$) and 89.1° ($d = 1.09$) which were assigned to the metallic Ni phase, and peaks with $2\theta = 19.9$ ($d = 4.60$), 32.0 ($d = 2.81$), 36.2 ($d = 2.41$), 46.9 ($d = 1.99$), 60.0 ($d = 1.52$), 61.1 ($d = 1.41$) and 83.5° ($d = 1.15$) which were assigned to the alumina phase.¹⁷

The XRD patterns of the fresh Ni/SiO₂ and the used Ni/SiO₂ catalysts are shown in Fig. 2. The broad diffraction peaks can be attributed to the presence of amorphous silica in the catalysts¹⁸ which is seen at $2\theta = 21.7^\circ$.

XRD analysis shows that the diffraction lines corresponding to the NiO are slightly sharper on the Ni/Al₂O₃ than on the Ni/SiO₂. This indicates the effect of the different support on the size of the Ni crystallites, with Al₂O₃ favouring better crystallinity and formation of larger Ni crystallites.^{19,15} The calculated Ni particle sizes (Scherrer equation), presented in Table 1, indeed show that Ni particles supported on Al₂O₃ were larger than Ni supported on SiO₂.

The sharpening of the Ni metal peaks in the XRD patterns of the used catalysts suggests improved crystallinity likely due to the sintering of the Ni particles.¹⁸ This supports the BET data.

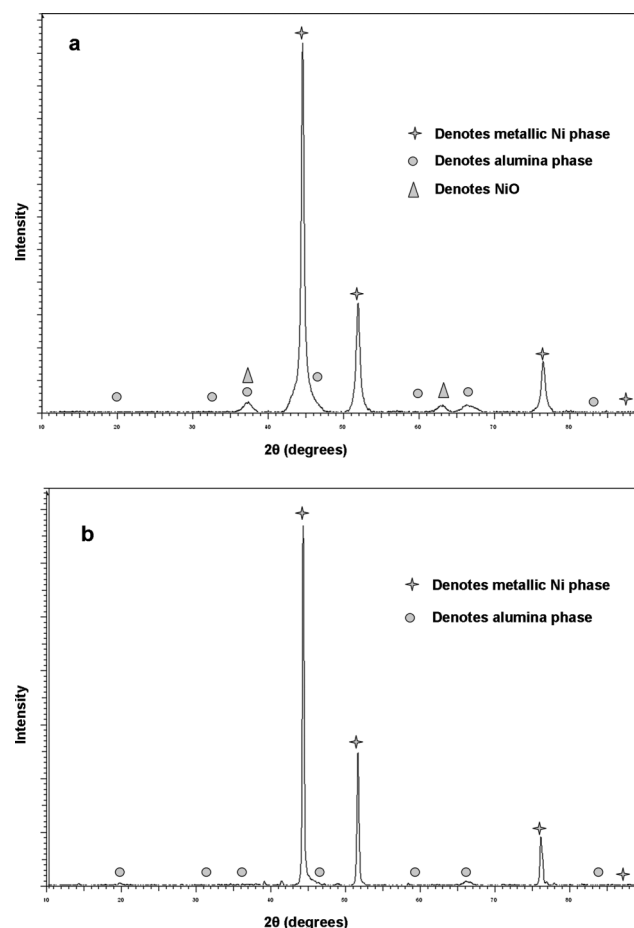


Fig. 1 (a): XRD pattern of the fresh Ni/Al₂O₃ catalyst. (b): XRD pattern of the used Ni/Al₂O₃ catalyst.

3.1.3 Temperature-programmed reduction. TPR characterisation is often used to analyse catalysts for surface Ni species, reducibility and metal-support interaction.²⁴ Fig. 3 shows the TPR profile of fresh Ni/Al₂O₃, and this catalyst exhibited five reduction peaks (198, 280, 570, 700 and 800 °C). Peaks observed at temperatures lower than 400 °C can be attributed to NiO not associated or weakly associated with the support. The reduction peaks at higher temperatures can be associated with the strong interaction of the NiO and the support. Rynkowski *et al.*²⁰ reported that the peak at 700 °C is representative of the reduction of nickel that had reacted with the support, forming nickel aluminate, NiAl₂O₄, and the peak at 800 °C is due to nickel aggregates.²¹ Feng *et al.*²² also confirmed that the peak at 700 °C is due to the reduction of a NiAl₂O₄ spinel or strongly interacting NiO- γ -Al₂O₃ phase.

Yang *et al.*²³ studied the effect of Ni loadings on the surface Ni species. They observed, most importantly, that the number of Ni species increased with increased Ni loading. The distinct difference in the number of reduction peaks indicates that the Ni loading has a prominent effect on the Ni species.

Fig. 4 shows the TPR profile for fresh Ni/SiO₂. The peak at 240 °C was due to highly dispersed NiO on the support. Mile *et al.*²⁴ assigned the peak at 336 °C to the nickel oxide with little or no interaction with the support, the peak at 520 °C

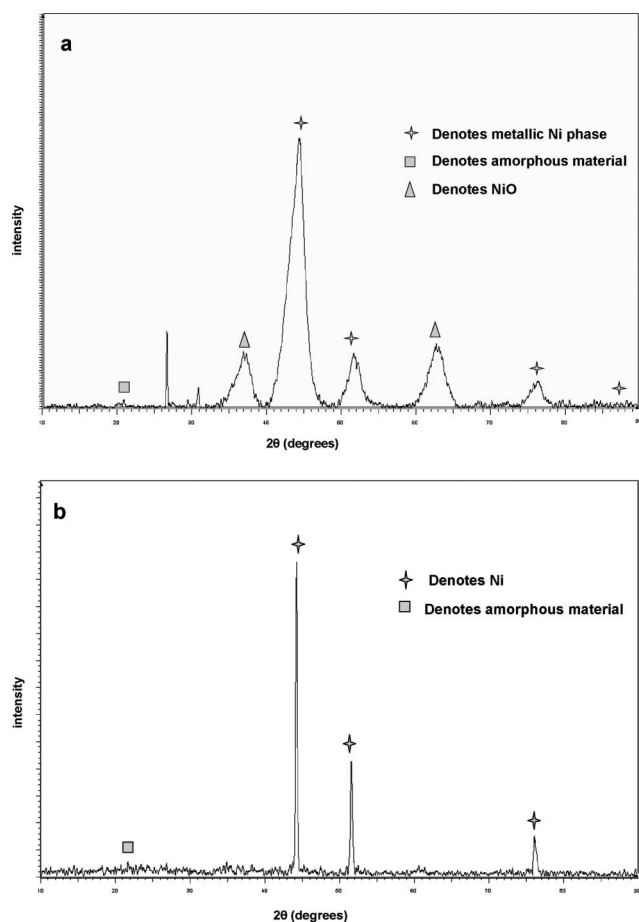


Fig. 2 (a): XRD pattern of the fresh Ni/SiO₂ catalyst. (b): XRD pattern of the used Ni/SiO₂ catalyst.

to the “free” nickel oxide, and the peak at 645 °C to a strong metal–support interaction.

3.1.4 Temperature-programmed desorption. The acidity of the alumina or silica plays an important role in hydrogenolysis. Table 2 gives a range of acid sites for the two different systems. The Ni/Al₂O₃ catalysts showed peaks at 182, 366 and 603 °C whereas, the Ni/SiO₂ catalyst showed peaks at 237, 368 and 662 °C. Pattamakomsan *et al.*²⁵ reported that their Al₂O₃ supported catalyst showed desorption peaks around 170 °C and 340 °C which corresponded to weak and medium acid sites respectively. An additional peak was observed near 600 °C indicating strong acid sites of the Al₂O₃ support. From Table 2 it is clear that the Ni/SiO₂ catalyst had a slightly higher total acidity, but showed a higher distribution of weak acid sites. The Ni/Al₂O₃ catalyst showed a higher content of strong acid sites.

3.1.5 Electron microscopy. Fig. 5 presents typical SEM images of the fresh and used Ni/SiO₂ catalysts. The SEM

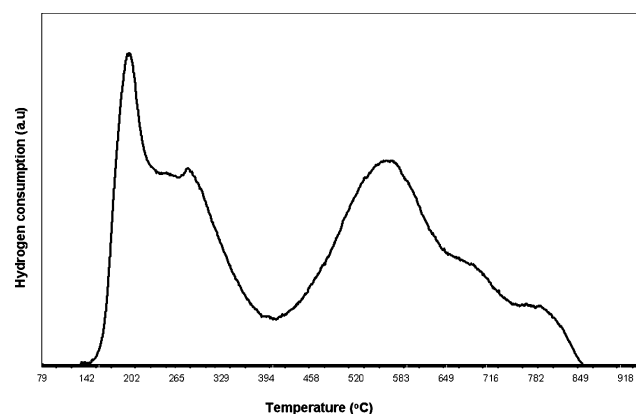


Fig. 3 TPR profile of fresh Ni/Al₂O₃ catalyst.

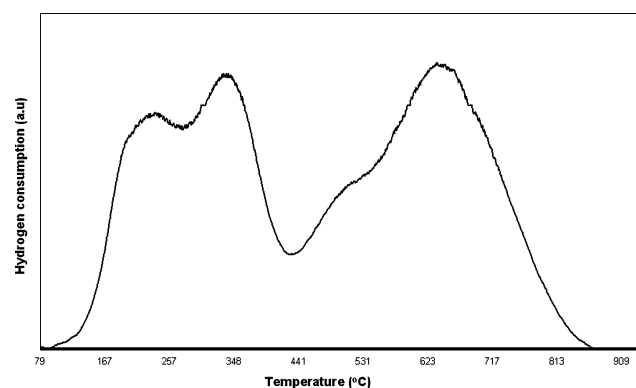


Fig. 4 TPR profile of fresh Ni/SiO₂ catalyst.

image of the fresh Ni/SiO₂ catalyst showed bright spots on the particles, which can be attributed to the Ni crystallites exposed on the surface.²⁶ The used Ni/SiO₂ catalyst showed large clusters, which can be attributed to sintering, and this was also reflected in the BET measurements.

Fig. 6 shows the TEM images of the fresh Ni/SiO₂ catalyst and the used Ni/SiO₂ catalyst. The fresh Ni/SiO₂ catalyst showed large spherical particles with smaller particles along the edges. The used Ni/SiO₂ catalyst has a thin sheet-like appearance with no distinct presence of spherical particles. Evidence of sintering is clearly visible in the TEM image, Fig. 6(b). The electron diffraction pattern (Fig. 7) of the fresh Ni/SiO₂ catalyst shows a ring pattern which is an indication of either an amorphous or polycrystalline nature of the catalyst. A ring pattern which is made up of spots usually implies small particle sizes, which were confirmed by XRD. The diffraction pattern of the used Ni/SiO₂ catalyst suggests greater crystallinity.

Table 2 Acidity of the Ni-supported catalysts

Catalyst	Acidity (mmol NH ₃ g ⁻¹)			
	Weak acid sites	Medium acid sites	Strong acid sites	Total acidity
Fresh Ni/Al ₂ O ₃	0.085	0.669	1.170	1.924
Fresh Ni/SiO ₂	0.942	0.852	0.381	2.175

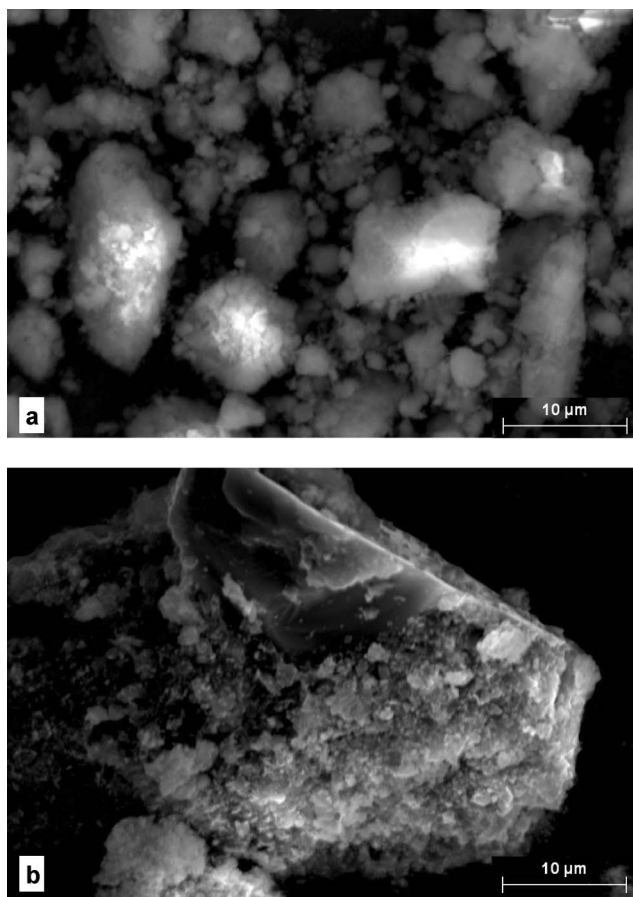


Fig. 5 (a): SEM image of the fresh Ni/SiO₂ catalyst. (b): SEM image of the used Ni/SiO₂ catalyst.

3.1.6 Thermogravimetric analysis. The thermogravimetric plots for both the fresh Ni/Al₂O₃ and Ni/SiO₂ catalysts are given in Fig. 8. The initial weight loss of about 7% up to 200 °C, for both unreduced catalysts, is attributed to the loss of water. A very slow but constant decrease in weight up to 700 °C was observed for both fresh catalysts, and can be attributed to the loss of organic materials from preparation.²⁷

Fig. 8 also shows the TGA curves for the used Ni/Al₂O₃ and Ni/SiO₂ catalysts. Again a weight loss was seen up to 200 °C, which was attributed to the loss of water. The Ni/Al₂O₃ catalyst showed a significant weight loss of 21.9% up to 700 °C. This can be due to the decomposition of by-products which are formed during the catalytic reaction and adsorb on the catalyst. The Ni/SiO₂ catalyst showed a weight loss of 9.9% up to 700 °C, and then a second weight loss of 8.3% up to 900 °C, which is due to the deposition of carbonaceous material.

The DSC plots for the fresh Ni/Al₂O₃ and Ni/SiO₂ catalysts are also shown in Fig. 8. For the Ni/Al₂O₃ catalyst, an initial small endothermic peak below 200 °C is attributed to the loss of water, which is supported by the corresponding weight loss in the TGA curve. A second small endothermic peak at about 300 °C can be due to the loss of more water or due to the loss of organic materials. An endothermic effect was observed for the Ni/SiO₂ catalyst corresponding to the dehydration of silica and water evaporation in the temperature range 60–400 °C.²⁸

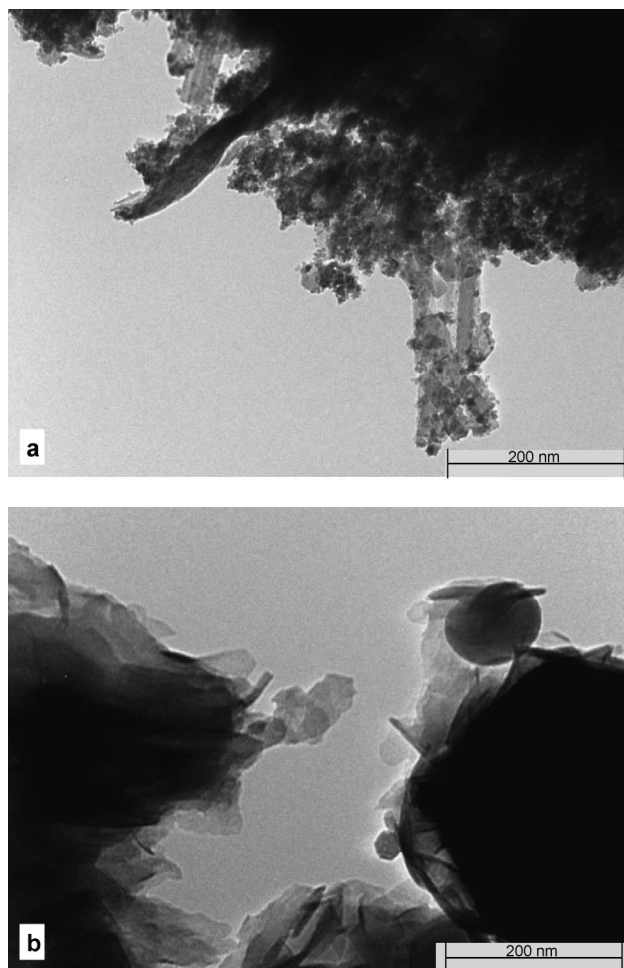


Fig. 6 (a): TEM images of the fresh Ni/SiO₂ catalyst. (b): TEM images of the used Ni/SiO₂ catalyst.

3.2 Catalytic testing

3.2.1 Effect of pressure on glycerol hydrogenolysis. The extent of hydrogenolysis using a Ni/SiO₂ catalyst, as a function of pressure at constant temperature (230 °C), is shown in Table 3. The data showed that pressure does not have a significant influence on the glycerol conversion as similarly observed by Dasari *et al.*,⁶ however, a change in the selectivities of the polyols was observed. The selectivity to the lower alcohols remained essentially unchanged. The products included 1,2-propanediol, acetol, ethylene glycol, ethanol and methane.

The main product observed during glycerol hydrogenolysis over the Ni/SiO₂ catalyst at the conditions expressed in Table 3 was 1,2-PDO. The selectivity to 1,2-PDO decreased with increasing hydrogen pressure from 78% to 67%. At low pressures, a selectivity of ~5% acetol was obtained, which decreased to 2% as the pressure increased. It is claimed that acetol is the intermediate in the formation of 1,2-PDO using acid catalysts *via* dehydration and subsequent hydrogenation.⁴ The selectivity to 1,2-PDO showed a decrease with increasing pressure to the advantage of EG. The higher EG selectivity is likely due to the degradation of 1,2-PDO to EG²⁹ at high H₂ pressures. It is also likely that the higher pressures favour direct hydrogenolysis of

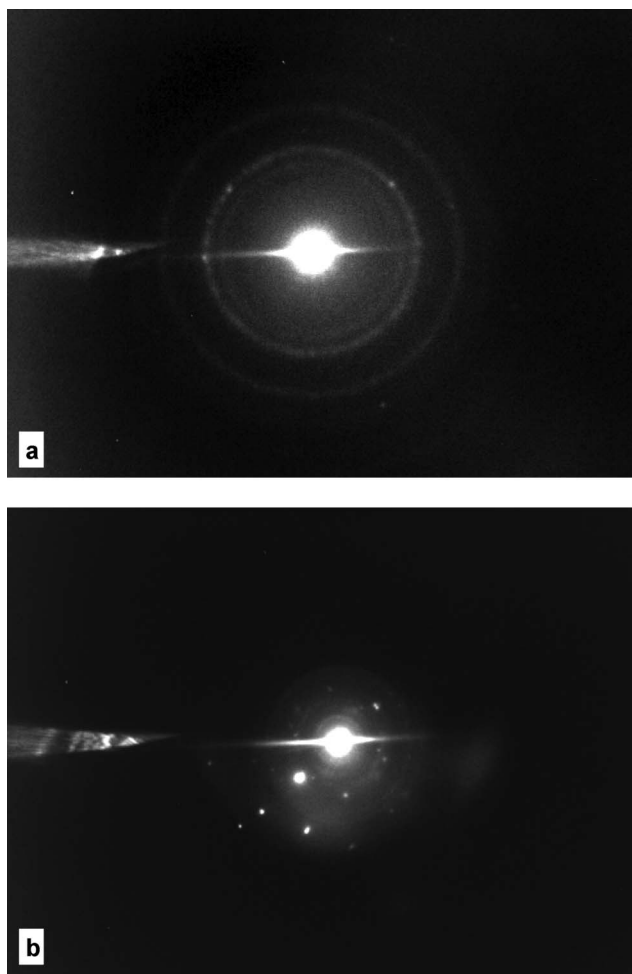


Fig. 7 (a): Electron diffraction patterns of the fresh Ni/SiO₂ catalyst. (b): Electron diffraction patterns of the used Ni/SiO₂ catalyst.

Table 3 Effect of pressure on glycerol hydrogenolysis over a Ni/SiO₂ catalyst at 230 °C

	Selectivities to different products (C mole basis)		
	40 bar H ₂	60 bar H ₂	75 bar H ₂
Methane	1.2	3.6	4.8
Methanol	1.3	1.7	2.1
Ethanol	5.5	5.4	4.2
1-Propanol	1.2	0.6	1.1
Acetol	4.5	4.1	1.9
Ethylene glycol	7.3	13.5	15.9
1,2-PDO	77.9	70.6	67.8
Others ^a	1.1	0.5	2.2
Conversion	14.5	16.2	13.0

^a Others = CO₂, 1,3-PDO, condensation products, unknowns.

glycerol to EG.⁴ The increase in methane selectivity also supports this pathway to EG.

3.2.2 Effect of temperature on glycerol hydrogenolysis.

Table 4 shows the conversion of glycerol and selectivity to products over the Ni/Al₂O₃ system as a function of temperature at constant pressure (60 bar). From the results at 230 °C, 1,2-PDO, acetol and ethanol were observed as the major products.

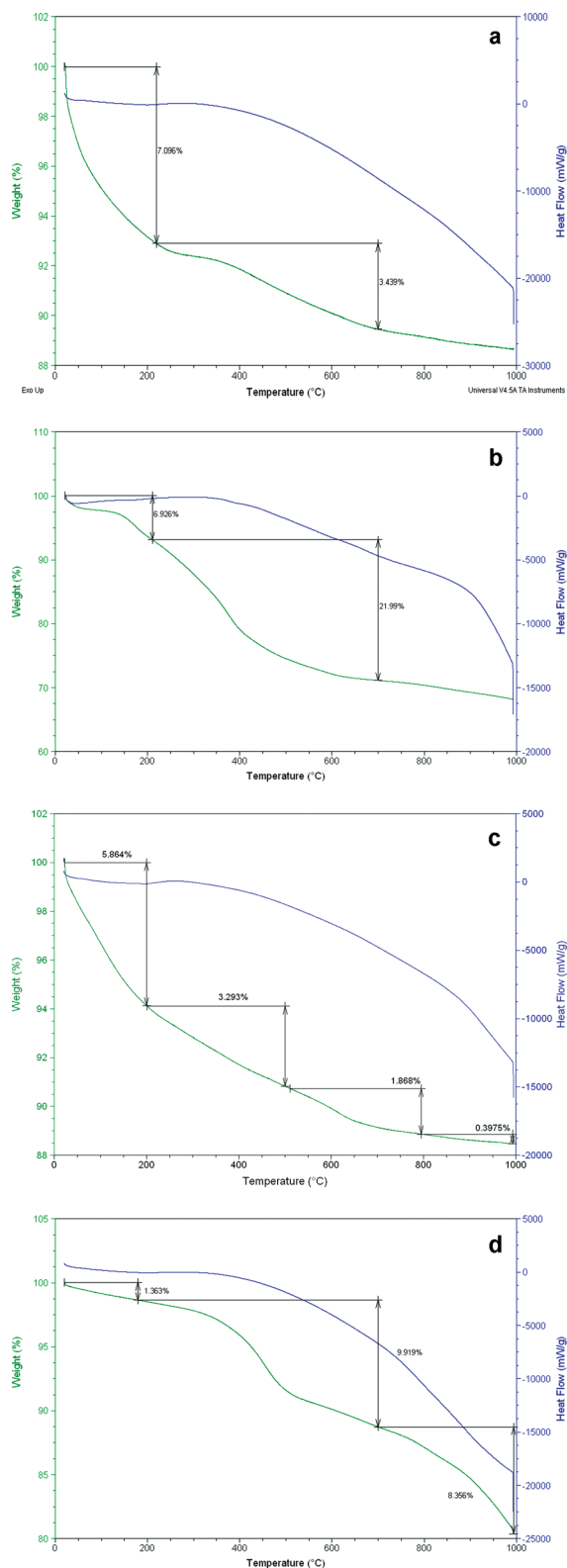


Fig. 8 (a): TGA-DSC curve of the fresh Ni/Al₂O₃ catalyst. (b): TGA-DSC curve of the used Ni/Al₂O₃ catalyst. (c): TGA-DSC curve of the fresh Ni/SiO₂ catalyst. (d): TGA-DSC curve of the used Ni/SiO₂ catalyst.

The conversion was observed to increase as the temperature increased from 230 °C to 320 °C. At 230 °C, the highest

Table 4 Effect of temperature on glycerol hydrogenolysis over a Ni/Al₂O₃ catalyst at 60 bar H₂

	Selectivities to different products (C mole basis)				
	230 °C	250 °C	275 °C	300 °C	320 °C
Methane	2.4	1.7	1.4	1.5	1.8
CO	0.0	0.0	0.2	2.0	3.2
CO ₂	0.3	0.4	0.2	1.2	2.0
Methanol	0.7	0.8	0.8	0.9	2.4
Ethanol	9.0	8.4	10.6	11.4	16.8
Acrolein	0.0	0.4	2.1	8.1	11.9
1-Propanol	0.5	2.4	12.1	24.4	35.3
Acetol	3.2	11.7	22.1	20.4	12.2
Ethylene glycol	3.1	1.0	1.2	1.0	0.4
1,2-Propanediol	79.9	70.2	36.7	12.1	1.8
1,3-Propanediol	0.0	0.3	4.8	6.2	2.2
Others ^a	0.9	2.7	7.8	10.8	10.0
Conversion	15.9	25.6	39.3	83.7	96.1

^a Others = ethane, propane, acetaldehyde, propenol, 2-propanol, condensation products, unknowns.

selectivity towards 1,2-PDO of 80% was achieved with a selectivity of 9% to ethanol.

As the temperature increased, the 1,2-PDO selectivity decreased from 80% to 2%, while an increase in ethanol selectivity was observed from 9% to 17%. At the same time, the 1-propanol selectivity was observed to increase to 35%, as were the selectivities to the dehydration products, acetol and acrolein. The heavier by-products also increased from <1% to 9% as the temperature increased.

The extent of hydrogenolysis using a Ni/SiO₂ catalyst, as a function of temperature at constant pressure (60 bar H₂), is shown in Table 5. The major products observed at 230 °C included 1,2-PDO, 1-propanol and ethanol.

The data showed that temperature again had a significant effect on the glycerol conversion. As the temperature of the reaction increased from 230 °C to 320 °C there was a uniform increase in the glycerol conversion from 16% to 99%. The overall selectivity to 1,2-PDO decreased significantly as the temperature

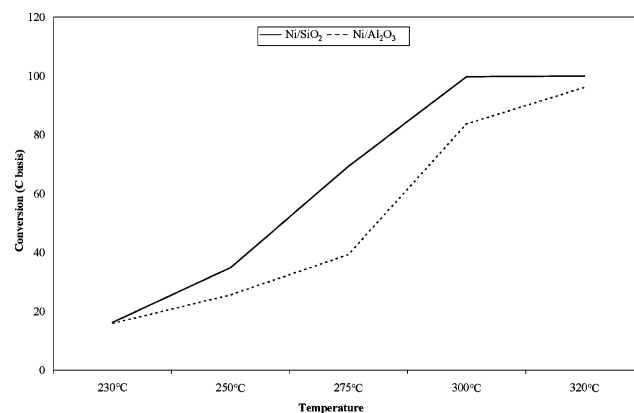
Table 5 Effect of temperature on glycerol hydrogenolysis over a Ni/SiO₂ catalyst at 60 bar H₂

	Selectivities to different products (C mole basis)				
	230 °C	250 °C	275 °C	300 °C	320 °C
Methane	3.6	2.8	2.1	2.6	3.0
CO	0.0	0.0	0.9	2.8	4.4
CO ₂	0.3	0.2	0.3	1.0	1.8
Methanol	1.7	1.3	1.5	2.7	5.5
Ethanol	5.4	6.6	12.4	16.9	20.2
Acrolein	0.0	0.0	1.1	2.6	3.9
1-Propanol	0.6	6.3	14.2	36.6	42.8
Acetol	4.1	3.8	12.4	7.7	4.2
Ethylene glycol	13.5	6.6	3.3	0.3	0.5
1,2-Propanediol	70.6	69.1	47.8	19.0	4.6
1,3-Propanediol	0.0	0.3	0.3	0.3	0.6
Others ^a	0.2	3.0	3.7	7.5	8.5
Conversion	16.2	34.9	69.3	99.8	99.9

^a Others = ethane, propane, acetaldehyde, propenol, 2-propanol, condensation products, unknowns.

was increased to 320 °C, which was accompanied by an increase in the selectivity to ethanol and propanol. A total selectivity of 69% to lower alcohols was obtained (methanol included). Higher temperatures also produced higher selectivity to gaseous products like methane, ethane, propane, carbon monoxide and carbon dioxide, as well as heavy constituents. This was also observed by Tomishige and co-workers,³⁰ where at higher reaction temperatures the selectivity to degradation products like ethanol, methanol and methane over SiO₂-supported catalysts increased significantly.

A conversion hysteresis (Fig. 9) was observed as temperature was increased from 230 °C to 320 °C, for the different catalysts, in favour of Ni/SiO₂.

**Fig. 9** Conversion hysteresis for Ni/SiO₂ and Ni/Al₂O₃ systems.

At 300 °C, a quantitative conversion was seen over the Ni/SiO₂, while a conversion of 83.7% was observed over the Ni/Al₂O₃ catalyst.

The higher activity of the Ni/SiO₂ catalyst can be ascribed to a higher density of Ni active sites for reaction. This is thought to occur because of a weaker metal–support interaction, and thus improved reducibility when compared to Ni/Al₂O₃, as suggested by the TPR data.

Although both sintering and carbon deposits could affect the activity of the catalyst over time, no significant deactivation of the catalysts was observed over a period of 72 h.

A possible explanation for the different product selectivities observed for the two systems can be related to metal–support interaction³¹ and the difference in acidity of the support.

The selectivity to 1,2-PDO (80%) was higher over the alumina-supported catalyst than over the silica-supported catalyst (71%) at similar conversion (~16%). This is likely due to the higher concentration of strong acid sites on the Ni/Al₂O₃ compared to Ni/SiO₂, which favoured the dehydration of glycerol to acetol and subsequent hydrogenation of acetol to 1,2-PDO.

A higher EG selectivity (13%) was observed over the Ni/SiO₂ catalyst than the Ni/Al₂O₃ catalyst, likely due to the higher propensity for C–C cleavage over the Ni/SiO₂ catalyst. It has been claimed that nickel has a strong ability for breaking C–C bonds, which can lead to shorter-chain products. More available Ni sites for the Ni/SiO₂ catalyst may suggest a reason for the higher EG selectivity for this system.

The selectivity to propanol and ethanol increased with increasing temperature, with a subsequent decrease in EG and

1,2-PDO selectivity. A similar trend was observed by Balaraju *et al.*²⁹ over a Ru/C catalyst. They observed that as the glycerol conversion increased, the selectivity to 1,2-PDO decreased and subsequently the selectivity to lower alcohols like ethanol and methanol increased. However, it is generally proposed that the formation of EtOH occurs most likely *via* 1,3-PDO.⁴ The low selectivity to 1,3-PDO observed may suggest that this is not necessarily the dominant pathway to EtOH. It is likely that due to the high concentration of 1,2-PDO present in the product, that this may be the likely intermediate to the propanols as well as EtOH.

As the conversion over the two systems increased, a higher propensity for dehydration was observed for the alumina-supported catalyst,³² whilst a higher hydrogenation rate was observed for the Ni/SiO₂ catalyst. This is shown in Table 6, which shows an increase in dehydration products, such as acrolein and acetol, for the Ni/Al₂O₃ and alcohols, such as ethanol and propanol, for Ni/SiO₂.

The lighter compounds, CH₄, CO and CO₂, showed a similar selectivity profile for both catalytic systems. The formation of CO and CO₂ is proposed to occur *via* decarbonylation reactions of aldehydic intermediates coupled to the water gas shift reaction. CH₄ likely forms *via* direct hydrogenation of CO or MeOH.

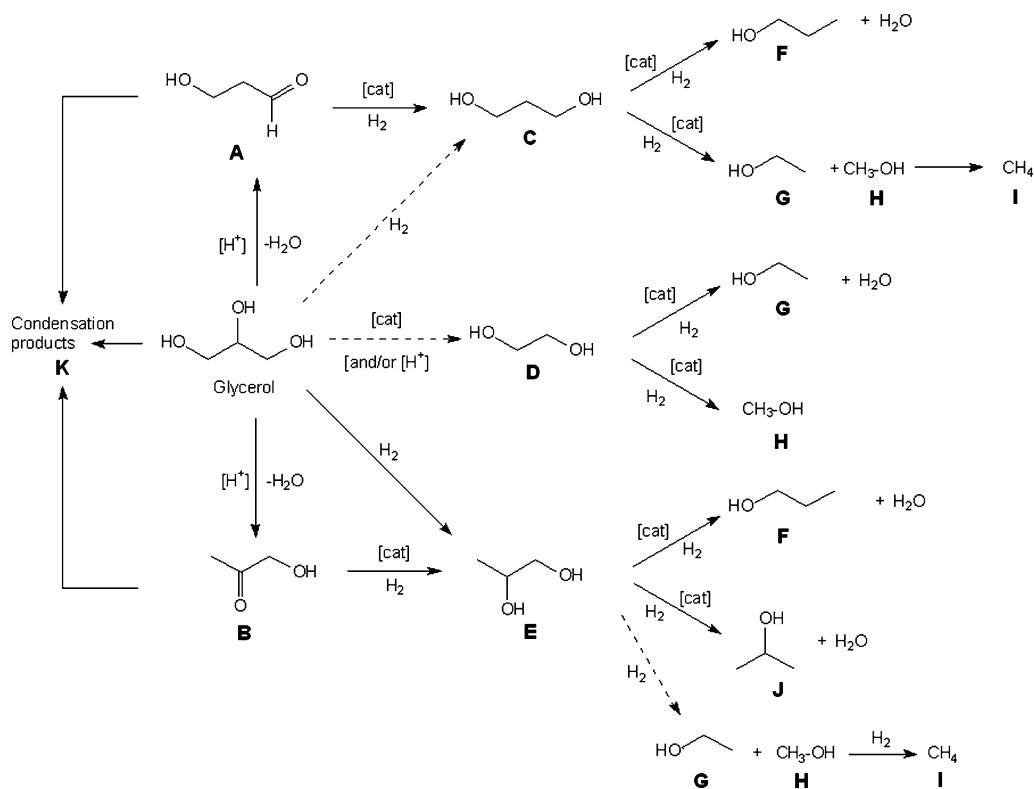
However, condensation to give heavier products, which included ethers and aldol type compounds, was more pronounced over the alumina-supported catalyst. This can be ascribed to an increased rate of condensation due to the higher (strong) acidity of the alumina support.

Table 6 Difference in product selectivities as a function of conversion over Ni/SiO₂ and Ni/Al₂O₃ systems

Catalyst	Conversion (%)	Product selectivities (%)	
		Alcohols ^a	Dehydration products ^b
Ni/Al ₂ O ₃	15.9	10.2	3.2
	25.6	11.6	12.1
	39.3	23.5	24.2
	83.7	36.7	28.5
	96.1	54.5	24.1
Ni/SiO ₂	16.2	8.6	0.1
	34.9	14.3	1.1
	69.3	28.1	3.7
	99.8	56.3	7.2
	99.9	68.5	8.5

^a Alcohols = methanol, ethanol and propanol. ^b Dehydration products = acetol, acrolein and propanol.

The possible transformation of glycerol can occur *via* several pathways as shown in Scheme 1.⁴ The first, resulting from acid-catalysed dehydration, can form 3-hydroxypropionaldehyde (A) and acetol (B), which can be subsequently hydrogenated to 1,3-PDO and 1,2-PDO respectively. It has been reported that glycerol can also be transformed *via* hydrogenolysis to form 1,3-PDO (C), EG (D) and 1,2-PDO (E),^{3,33,34} although some authors are of the opinion that these routes are not direct routes.^{35,36} The subsequent diols can undergo further hydrogenolysis to form primary alcohols such as 1-propanol (F), ethanol (G) and methanol (H), as well as secondary alcohols like isopropanol (J).⁴ C₁ products such as methane (I), CO and CO₂ can form *via*



Scheme 1 Reaction scheme showing glycerol transformation.

decomposition reactions or the water gas shift reaction. Heavier products can form *via* condensation reactions of glycerol or the aldehydic intermediates. In addition to the pathways described in Scheme 1, we propose that ethanol is also likely to form *via* 1,2-PDO.

4. Conclusion

The effect of increasing pressure was observed to have little influence on glycerol conversion. However, the selectivity to 1,2-PDO decreased with increasing pressure while EG and CH₄ selectivity was observed to increase. The selectivity to lower alcohols remained essentially unchanged.

Temperature was observed to have a significant effect on the glycerol conversion with Ni/SiO₂, giving a higher conversion than Ni/Al₂O₃ except at the lowest temperature studied. With respect to selectivity, 1,2-PDO was dominant at low temperature, whilst alcohols such as propanol, ethanol and methanol dominated the product profile at higher temperature. At 320 °C, a quantitative conversion of glycerol was observed, with a total selectivity of 69% to lower alcohols which included 1-propanol, ethanol and methanol. To the best of our knowledge, this is the highest selectivity reported to lower alcohols from glycerol using a continuous-flow fixed-bed reactor with an inexpensive catalytic system.

The pathway to the lower alcohols is proposed to occur *via* degradation of the intermediate polyols such as 1,2-PDO, 1,3-PDO and possibly EG. A mechanistic study is in progress to establish the route to the lower alcohols *via* glycerol.

Comparison of the product selectivity of the two catalysts revealed that the intrinsic properties of the support, such as the acidity of the support and the metal–support interaction, may have had an influence.

Acknowledgements

All catalytic work was performed at Sasol Technology Research and Development, and catalyst characterisation was carried out at the University of KwaZulu-Natal. We would also like to thank the Electron Microscope Unit as well as the Catalysis Research Group at the University of KwaZulu-Natal for the help with the characterisation data.

References

- 1 Y. Zheng, X. Chen and Y. Shen, *Chem. Rev.*, 2008, **108**, 5253–5277.
- 2 T. Hirai, N. Ikenaga, T. Miyake and T. Suzuki, *Energy Fuels*, 2005, **19**, 1761–1762.
- 3 J. Chaminand, L. Djakovitch, P. Gallezot, P. Marion, C. Pinel and C. Rosier, *Green Chem.*, 2004, **6**, 359–361.

- 4 T. Miyazawa, Y. Kusunoki, K. Kunimori and K. Tomishige, *J. Catal.*, 2006, **240**, 213–221.
- 5 R. Garcia, M. Besson and P. Gallezot, *Appl. Catal., A*, 1995, **127**, 165–176.
- 6 M. A. Dasari, P. P. Kiatsimkul, W. R. Sutterlin and G. J. Suppes, *Appl. Catal., A*, 2005, **281**, 225–231.
- 7 P. Bloom, Archer Daniels Midland Company, US 0103339 (2008).
- 8 R. Bullock, P. J. Fagan, E. M. Hauptman and M. Schalf (E. I. Du Pont de Nemours and company), *World Pat.* WO 98241, 2001.
- 9 L. Huang, Y. L. Zhu, H. Y. Zheng, Y. W. Li and Z. Y. Zeng, *J. Chem. Technol. Biotechnol.*, 2008, **83**, 1670–1675.
- 10 E. Drent and W. W. Jager (Shell Oil Company), *US Pat.* 6080898, 2000.
- 11 I. Furikado, T. Miyazawa, S. Koso, A. Shimao, K. Kunimori and K. Tomishige, *Green Chem.*, 2007, **9**, 582–588.
- 12 P. D. Pavlechko, *PEP Report No. 268: Higher alcohols from syngas*, SRI Consulting, 2009.
- 13 E. Linak, *CEH Marketing Research Report: Ethanol*, 2009.
- 14 S. Bizarri, M. Blagoev, and H. Mori, *CEH Marketing Research Report: Glycerin*, 2008.
- 15 E. S. Vasiladou, E. Heracleous, I. A. Vasalos and A. A. Lemonidou, *Appl. Catal., B*, 2009, **92**, 90–99.
- 16 S. Rakass, H. Oudghiri-Hassani, P. Rowntree and N. Abatzoglou, *J. Power Sources*, 2006, **158**, 485–496.
- 17 S. Shang, G. Liu, X. Chai, X. Tao, X. Li, M. Bai, W. Chu, X. Dai, Y. Zhao and Y. Yin, *Catal. Today*, 2009, **148**, 268–274.
- 18 Z. Huang, F. Cui, H. Kang, J. Chen and C. Xia, *Appl. Catal., A*, 2009, **366**, 288–298.
- 19 A. Saadi, R. Merabti, Z. Rassoul and M. M. Bettahar, *J. Mol. Catal. A: Chem.*, 2006, **253**, 79–85.
- 20 J. M. Rynkowski, T. Paryjczak and M. Lenik, *Appl. Catal., A*, 1993, **106**, 73–82.
- 21 P. Kim, Y. Kim, H. Kim, I. K. Song and J. Yi, *J. Mol. Catal. A: Chem.*, 2005, **231**, 247–254.
- 22 J.-T. Feng, Y.-J. Lin, D. G. Evans, X. Duan and D.-Q. Li, *J. Catal.*, 2009, **266**, 351–358.
- 23 R. Yang, X. Li, J. Wu, X. Zhang, Z. Zhang, Y. Cheng and J. Gou, *Appl. Catal., A*, 2009, **368**, 105–112.
- 24 B. Mile, D. Striling and M. A. Zammitt, *J. Mol. Catal.*, 1990, **62**, 179–198.
- 25 K. Pattamakomsan, K. Suriye, S. Dokjampa, N. Mongkolsiri, P. Praserttham and J. Panpranot, *Catal. Commun.*, 2010, **11**, 311–316.
- 26 A. E. Aksoylu, Z. Misirli and Z. I. Onsan, *Appl. Catal., A*, 1998, **168**, 385–397.
- 27 D. N. Srivastava, N. Perkas, G. A. Seisenbaeva, Y. Koltypin, V. G. Kessler and A. Gedanken, *Ultrason. Sonochem.*, 2003, **10**, 1–9.
- 28 G. A. Sharpataya, G. P. Panasyuk, G. P. Budova, Z. P. Ozerova, I. L. Voroshilov and V. B. Lazarev, *Thermochim. Acta*, 1985, **93**, 271–274.
- 29 M. Balaraju, V. Rekha, P. S. Sai Prasad, B. L. A. Prabhavathi Devi, R. B. N. Prasad and N. Lingaiah, *Appl. Catal., A*, 2009, **354**, 82–87.
- 30 I. Furikado, T. Miyazawa, S. Koso, A. Shimao, K. Kunimori and K. Tomishige, *Green Chem.*, 2007, **9**, 582–588.
- 31 L. Huang, J. Xie, R. Chen, D. Chu and A. T. Hsu, *Mater. Res. Bull.*, 2010, **45**, 92–96.
- 32 R. J. J. Nel and A. de Klerk, *Ind. Eng. Chem. Res.*, 2009, **48**, 5230–5238.
- 33 I. Gandarias, P. L. Arias, J. Requies, M. B. Guemez and J. L. G. Fierro, *Appl. Catal., B*, 2010, **97**, 248–256.
- 34 J. Chaminand, L. Djakovitch, P. Gallezot, P. Marion, C. Pinel and C. Rosier, *Green Chem.*, 2004, **6**, 359–361.
- 35 C. Montassier, J. C. Menezo, L. C. Hoang, C. Renaud and J. Barbier, *J. Mol. Catal.*, 1991, **70**, 99–110.
- 36 E. P. Maris and R. J. Davis, *J. Catal.*, 2007, **249**, 328–337.